31st Annual International Conference of the IEEE EMBS
Minneapolis, Minnesota, USA, September 2-6, 2009

Capacitive on-line hematocrit sensor design based on Impedance Spectroscopy for use in hemodialysis machines

Dennis Trebbels, David Hradetzky, and Roland Zengerle

Abstract— **This paper presents a new design for an on-line and in-line hematocrit (HCT) sensor. Special feature of the sensor is the capability to measure the hematocrit of a blood sample inside standard plastic tubing widely used in medical equipment. No blood sample has to be extracted out of existing extracorporeal blood circulation systems such as hemodialysis machines or heart-lung machines. The sensor principle is based on electrical impedance spectroscopy. Dielectric properties of the blood and the plastic tubing are measured at various frequencies. In order to optimize the sensitivity, a unique electrode configuration is developed and optimized by Finite Element Simulation. The new electrode design optimizes the overall sensitivity of the sensor towards a change in dielectric properties of the blood caused by the HCT value and therefore decreases the sensitivity to side effects caused by temperature drift and component tolerances. As a result of the optimized overall sensor performance the complexity of a sensor readout circuitry can be reduced to a minimum which leads to an unmatched price-performance ratio for a complete measurement system.**

I. Introduction

Measuring the proportion of blood volume occupied by red blood cells, the so-called hematocrit value (HCT-value), is a major concern in many health care situations [1, 2]. This article focuses on situations where an extracorporeal blood circulation system is already available such as hemodialysis or heart-lung machines. In general there are many approaches to measure the HCT value of a blood sample based on different physical effects [3, 4]. One of the best-known methods is traditional centrifugation. Major drawback of this method is the fact that a blood sample has to be extracted out of an existing extracorporeal closed loop blood circulation system. Due to the time required for centrifugation this method is not suitable for continuous on-line measurement. Another well-known measurement method is based on turbidimetry using a photometer device. For this purpose a blood sample also has to be extracted out of the existing extracorporeal circulation system. The blood sample is mixed with reagent and then measured. Although this method is less time consuming than centrifugation, it still takes too long for an on-line measurement system. Furthermore both abovementioned methods require to extract a blood sample out of the closed loop system which causes additional risk of infection. In order to compensate for the mentioned drawbacks, new concepts for innovative on-line and in-line measurement devices have been developed [5, 6, 7, 8, 9, 10]. Primary objective of most new sensor concepts is to eliminate the requirement for extracting a blood sample out of a closed loop system. This strategy is preferred since no direct contact to the blood is required and the existing tubing on the machines remains closed and therefore is kept sterile.

One well-known HCT estimation method is based on optical measurement principles. Drawback of this method is the fact that a high-quality optical device has to be inserted into the existing plastic tubing which contains the blood. Inserting an additional device into the tubing causes additional effort to ensure a sterile system. Furthermore the expensive high-quality optical device must be a disposable because of the direct contact to the blood.

Another promising approach is estimating the HCT value based on electrical impedance spectroscopy [11, 12, 13]. This paper introduces a new sensor design for impedance spectroscopy based on multiple ring electrodes attached to the plastic tubing as shown in Fig. 1. The so formed capacitive sensor is used to measure the permittivity of the blood and the tubing walls at various frequencies. The obtained impedance spectrum is analyzed and the HCT value is calculated. The described new electrode design has been simulated and optimized using Finite Element Simulation. The result was verified by comprehensive experiments in the laboratory using pork blood. The result of the experiments is an optimized measurement frequency at which the sensitivity of the sensor towards the HCT value of the blood sample is at its optimum.

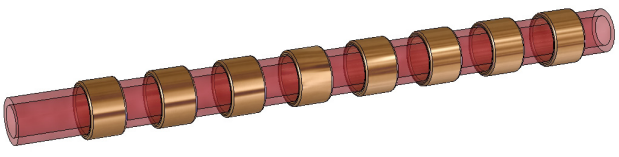

Fig. 1: New electrode design for the on-line hematocrit sensor. Each electrode is designed as a ring. The width and the distance of the electrodes is optimized for the given tubing dimensions by Finite Element Simulation. The overall sensor length is limited to 10 cm in the given application which results in a total number of 9 electrodes.

Manuscript received April 7, 2009.

Dennis Trebbels, HSG-IMIT, Institut für Mikro- und Informationstechnik der Hahn-Schickard-Gesellschaft e.V., 78052 Villingen-Schwenningen, Germany (phone: +49-7721-943-153; fax: +49-7721-943-210; e-mail: dennis.trebbels@hsg-imit.de).

David Hradetzky, HSG-IMIT, Institut für Mikro- und Informationstechnik der Hahn-Schickard-Gesellschaft e.V., 78052 Villingen-Schwenningen, Germany (phone: +49-7721-943-192; fax: +49-7721-943-210; e-mail: david.hradetzky@hsg-imit.de).

Roland Zengerle, Laboratory for MEMS-Applications, IMTEK, Department of Microsystems Engineering, University of Freiburg, Georges-Köhler-Allee 103, 79110 Freiburg, Germany (e-mail: zengerle@imtek.de)

II. Sensor Concept and Simulation

A. Sensor Principle

The new sensor estimates the HCT value of the blood inside the plastic tubing by measuring the overall sensor capacitance at various frequencies. The obtained impedance spectrum is then analyzed and the HCT value is calculated. Fig. 2 shows the connection of the electrodes to the measurement device. Adjacent electrodes always have opposite polarity. This design allows for implementing multiple capacitors by using multiple ring electrodes which are connected in parallel to the measurement device. This design increases the overall sensor capacitance to a maximum for a given overall length of the sensor.

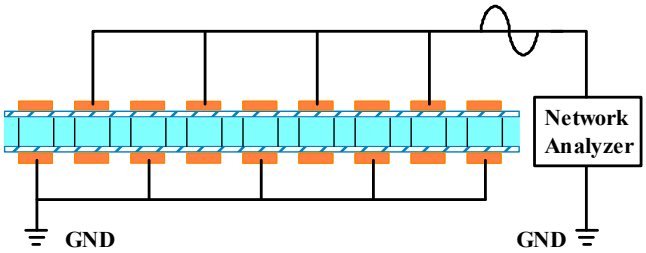

Fig. 2: The section view of the sensor shows the connection of the electrodes to the measurement equipment. Adjacent electrodes always have opposite polarity.

The measured overall capacitance is composed of several capacitive effects. Fig. 3 (A) illustrates the three major effects. Capacitor C1 represents the stray capacitance in air, C2 represents a capacitance between two electrodes influenced by the permittivity of the tubing wall material and C3 represents the capacitance between two electrodes depending on the properties of the blood inside the tubing. All three capacitive effects can be modeled by an equivalent electrical schematic as shown in Fig. 3 (B). The overall capacitance of the sensor is a parallel connection of C1, C2 and C3. Assuming a fixed geometry and stable material properties of the plastic tubing, only C3 will change its capacitance depending on the dielectric blood properties affected by the HCT value. Optimization of the electrodes is done by Finite Element Simulations.

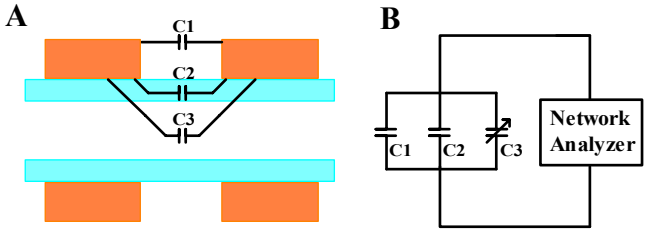

Fig. 3: Detailed view of one electrode pair. (A) Capacitor C1 represents the stray capacitance within air between two adjacent electrodes. C2 represents the capacitance between two electrodes influenced by the permittivity of the tubing material. C3 represents the capacitance influenced by the properties of the blood. (B) Equivalent electrical schematic for the three capacitive effects.

B. Simulation

In order to optimize the sensitivity of the sensor, the shape of the ring electrodes has to be optimized and adapted to the given dimensions of the plastic tubing. Finite Element Simulation of the electrical field pattern inside the sensor has been done. The graphical simulation results in Fig. 4 show a strong field distortion caused by the high permittivity of the blood and the relatively low permittivity of the plastic tubing walls. Fig. 4 (A) shows a normal field pattern as expected. The simulation was done with no blood inside the plastic tubing. Fig. 4 (B) shows the distorted field pattern for the real situation with blood inside the tubing. Due to this field distortion, the electrical field strength inside the tubing walls is approximately ten times higher than inside the blood and therefore causes a large sensor offset. Referring to Fig. 3 the modeled capacitor C2 is large compared to C1 and C3.

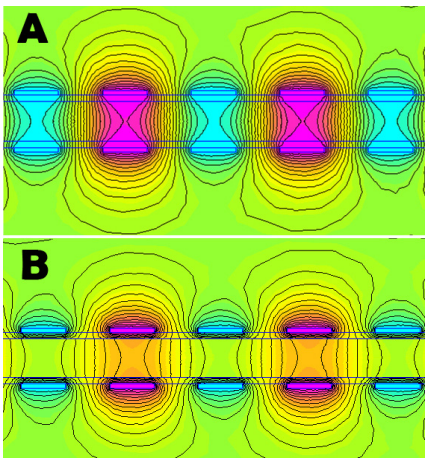

Fig. 4: Section view of the electrical field pattern of the sensor electrodes. (A) shows the field pattern for the plastic tubing filled with air. (B) shows the distorted field pattern for the tubing filled with blood.

The large sensor offset is a result of the tubing wall material and can not be fully eliminated. Since the geometry of the plastic tubing is given by the application, the goal of the simulation is to find a reasonable ratio between the distance of the electrodes and the width of each electrode. Both parameters have been investigated in parallel in Finite Element Simulations. For the simulation the following parameters of the tubing have been used: the tubing consists of PVC and therefore has a relative permittivity of approximately 2. The inner diameter of the tubing is 4.8 mm and the outer diameter is 6.4 mm. The simulation result for electrodes having a width of 5 mm is shown in Fig. 5. One graph shows the relative change of the sensor signal as a function of the distance between two adjacent electrodes. The second graph shows the overall capacitance of the sensor. Since the overall capacitance of the sensor is just in the range of a few pF, major goal of the simulation is to find a reasonable compromise between the sensitivity and the overall capacitance.

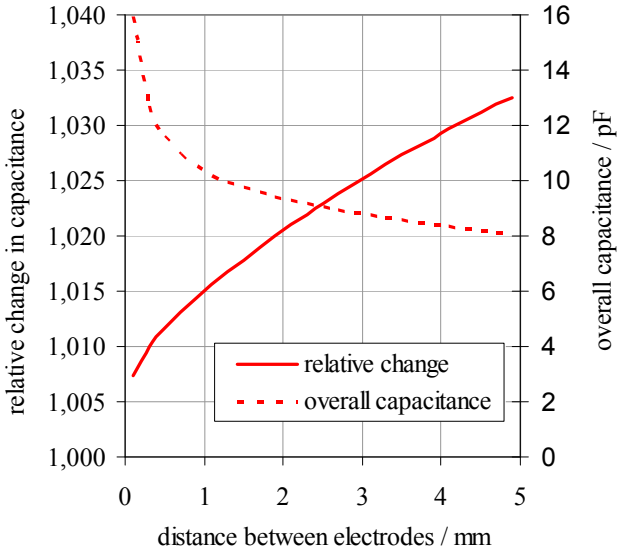

Fig. 5: Finite Element Simulation result for an electrode width of 5 mm. The solid line shows the relative change in capacitance as a function of the distance between two adjacent electrodes for an assumed change in permittivity from 80 down to 70 for the medium inside the tubing. The dashed line shows the overall sensor capacitance.

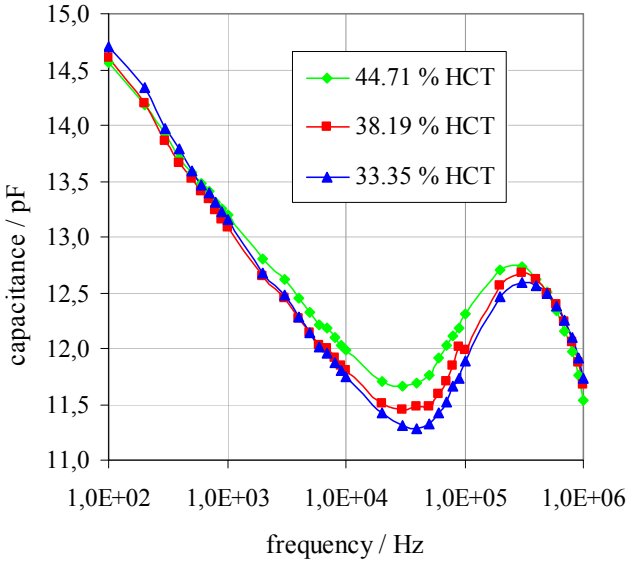

Fig. 6: Measurement results of the experiments in the laboratory using pork blood. The three graphs show the overall sensor capacitance as a function of the frequency. For reference the HCT values of the blood samples have been measured with a conventional photometer.

On the one hand the two graphs in Fig. 5 show that a small distance between the electrodes causes a large overall sensor capacitance but only a poor sensitivity. Referring to Fig. 3 this can be explained by an increased C1 as well as an increased C2. Large values for C1 and C2 cause an additional sensor offset signal and therefore minimize the relative change in capacitance. On the other hand a large distance between two electrodes causes an optimized sensitivity but the sensor will have a relatively low overall capacitance which makes it difficult to measure the low absolute values. In this particular case a reasonable compromise between both scenarios has been chosen and the distance between two adjacent electrodes is set to 3 mm.

III. Measurement Results

The sensor operation theory and the simulation result have been verified in the laboratory. Multiple experiments with pork blood have been done. The pork blood was centrifuged and a dilution series with plasma was prepared in order to obtain blood samples with different HCT values. The prepared blood samples have been measured inside a sensor prototype as shown in Fig. 1 and Fig. 2. The measurement was performed by a programmable RLC-Analyzer (Fluke PM6306). As a reference method a conventional photometer (Diaglobal Vario Photometer DP 300) has been used. The result of the experiments is presented in Fig. 6. The three graphs show the measured overall capacitance of the sensor as a function of the measurement signal frequency. The HCT value has been varied for each measurement sweep in order to investigate the frequency dependency.

The measurement results presented in Fig. 6 show an optimized measurement frequency in the range of approximately 40 kHz. At this particular frequency the relative change of the capacitance depending on the HCT value is significantly higher than at lower or higher frequencies. In other words the sensitivity of the sensor is optimized if the measurement frequency is 40 kHz. The relation between the HCT value and the capacitance at this frequency is presented in Fig. 7. The graph is almost linear and therefore allows an easy calculation of the HCT value for a measured capacitance. The gradient of the graph shown in Fig. 7 is approximately 33 fF per 1 % HCT value.

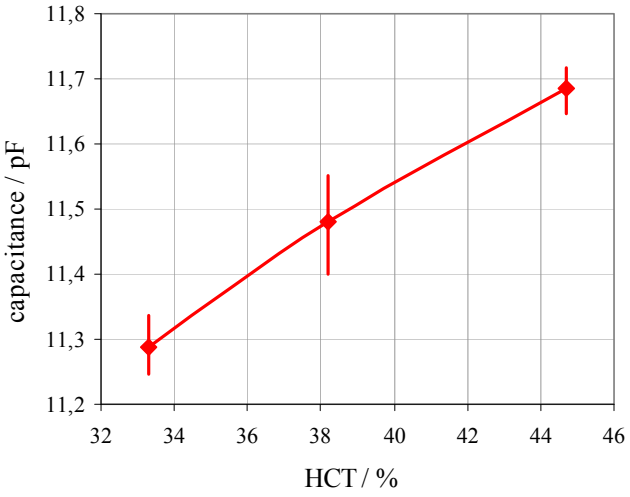

Fig. 7: Measurement results for a measurement frequency of 40 kHz. The graph shows the overall sensor capacitance as a function of the HCT value. The gradient of the graph is 33 fF per 1 % HCT. The measurement has been done in the laboratory using pork blood samples.

The existence of an optimized measurement frequency of 40 kHz can be explained by a simplified model of a single blood cell inside the sensor as shown in Fig. 8.

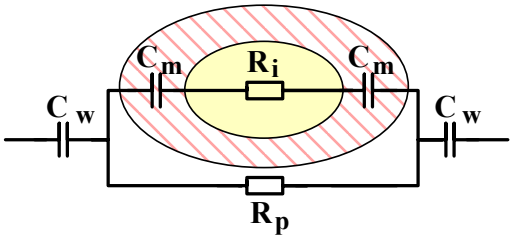

Fig. 8: Simplified electrical model of a single red blood cell inside the blood plasma. The cell membrane is modeled by the capacitors C_m, the inner cell volume is modeled by R_i. The blood plasma resistance is modeled by R_p and the capacitive coupling to the ring electrodes through the tubing walls is modeled by the capacitors C_w.

At low frequencies the capacitive cell membrane C_m is high impedant and therefore all current coupled via the tubing wall capacitors C_w flows through the blood plasma R_p. For increasing frequencies the cell membrane impedance drops down and a part of the current will now flow through the inner volume R_i of the cell. At a frequency of approximately 40 kHz the relative impedance change of the cell membrane in relation to the plasma resistance R_p and the inner resistance R_i is high which makes the model in Fig. 8 "sensitive" to frequencies in the range of 40 kHz. At very high frequencies the cell membrane impedance drops down to values negligible compared to the inner resistance and the plasma resistance. The cell membrane C_m in the model can then simply be replaced by a short circuit. In reality the described model of a single cell inside the sensor must be replaced by a series of cells which are capacitively coupled to each other. Fig. 9 illustrates this model by showing a few red blood cells inside the sensor capacitively coupled to the sensor electrodes through the tubing walls.

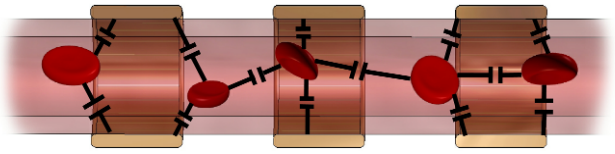

Fig. 9: Multiple red blood cells inside the sensor illustrate the capacitive coupling to each other and to the sensor electrodes via the tubing walls. The red blood cells are not true to scale but illustrate the general model of a series of single cells inside the sensor.

IV. Conclusions

This paper presents a new sensor design for measuring the HCT value of a blood sample. Special feature of the developed sensor design is the capability of measuring the HCT value inside standard plastic tubing widely used in medical equipment. Due to the sensor design there is no requirement for extracting a blood sample out of an existing extracorporeal blood circulation system. Advantage of the new sensor concept is the fact that no additional disposables are required for measuring the HCT value and no components of the sensor system have direct contact to the blood. The complete existing tubing remains sterile which drastically reduces the risk of an infection. The introduced sensor is intended for being used in hemodialysis machines and can simply be added to existing machines without any modifications to the machine or the existing tubing.

The new sensor concept is based on a frequency depending behavior of the blood inside the sensor. Experiments in the laboratory using impedance spectroscopy methods show the optimized measurement frequency of 40 kHz. A simplified model was found which confirms the measured values. At the optimum frequency the proposed sensor design achieves an optimized output signal. The sensitivity at this frequency is approximately 33 fF per 1 % HCT which allows for a relatively easy sensor readout circuitry and therefore a low overall measurement system cost.

References

[1] J. Z. Ma, J. Ebben, H. Xia, and A. J. Collins, "Hematocrit level and associated mortality in hemodialysis patients," *J. Amer. Soc. Nephrol.*, vol. 10, pp. 610-619, 1999

[2] A. Aris, J. M. Padro, J. O. Bonnin, and J. M. Caralps, "Prediction of hematocrit changes in open-heart surgery without blood transfusion," *J. Cardiovasc. Surg.*, vol. 25, no. 6, pp. 545-548, 1984

[3] M. Y. Jaffrin and C. Fournier, "Comparison of optical, electrical, and centrifugation techniques for haematocrit monitoring of dialyzed patients," *Med. Biol. Eng. Comput.*, vol. 37, no. 4, pp. 433–439, July 1994

[4] G. Wennecke, "Hematocrit – A review of different analytical methods," *Radiometer Medical ApS*, 2004

[5] K. Michihiro, M. Kosuke, N. Masamichi, T. Shigeo, T. Shinobu, and Y. Kenichi,"Development of noninvasive measurement method of blood hematocrit and oxygen saturation based on photoplethysmography," *IEIC Technical Report*, Vol. 106, No. 80, pp. 9-12, 2006

[6] W. Secomski, A. Nowicki, R. Olszewski, J. Adamus, P. Fidanzati, and P. Tortoli, "Doppler Multigate Measurements of Ultrasonic Scattering, Attenuation and Hematocrit of Blood in the Human Artery," *IEEE Ultrasonics Symposium,* 2005

[7] M. Karkar, W. M. Long, S.O. Heinemann, "Hematocrit measuring apparatus," United States Patent 4745279

[8] T. Ishihara, H. Inagaki, "Hematocrit measuring instrument," United States Patent 4484135, 1984

[9] R. G. Billings, J. S. Clark, K. Yang, J. Neese, A. L. Kaminsky, "System and method for in-vivo hematocrit measurement using impedance and pressure plethysmography", United States Patent 6128518, October 2000

[10] C. L. Davis, P. D. Harrison, J. E. Johnson, "Noninvasive method of measuring blood density and hematocrit," United States Patent 7011631, March 2006

[11] E. F. Treo, C. J. Felice, M. C. Tirado, M. E. Valentinuzzi, and Daniel O. Cervantes, "Hematocrit Measurement by Dielectric Spectroscopy," *IEEE Trans. On. Biomed. Engin.*, vol. 52, no. 1, 2005

[12] M. Fenech, M. Maasrani, and M. Y. Jaffrin, "Fluid Volumes Determination by Impedance Spectroscopy and Hematocrit Monitoring: Application to Pediatric Hemodialysis," *Artificial Organs*, vol. 25, no. 2, pp.89-98, 2001

[13] D. Trebbels, D. Hradetzky, S. Messner, and R. Zengerle, "Concepts for Non-Contact Hematocrit Measurement based on high precision Impedance Spectroscopy at low cost," *ISEMA09 proceedings*, accepted, 2009